

Ateneo de Manila University

Archium Ateneo

Physics Faculty Publications

Physics Department

2-27-2020

Non-tropical Cyclone Related Winter Heavy Rainfall Events over the Philippines: Climatology and Mechanisms

Gemma T. Narisma

Ateneo de Manila University, gnarisma@ateneo.edu

Jun Matsumoto

Tokyo Metropolitan University, Tokyo

Julie Mae Dado

Manila Observatory, Philippines

Lyndon Mark Olaguera

Ateneo de Manila University

Follow this and additional works at: <https://archium.ateneo.edu/physics-faculty-pubs>



Part of the [Oceanography and Atmospheric Sciences and Meteorology Commons](#), and the [Physics Commons](#)

Recommended Citation

Olaguera, L. M., Matsumoto, J., Dado, J. M. B., & Narisma, G. T. T. (2021). Non-tropical cyclone related winter heavy rainfall events over the Philippines: Climatology and mechanisms. *Asia-Pacific Journal of Atmospheric Sciences*, 57(1), 17–33. <https://doi.org/10.1007/s13143-019-00165-2>

This Article is brought to you for free and open access by the Physics Department at Archium Ateneo. It has been accepted for inclusion in Physics Faculty Publications by an authorized administrator of Archium Ateneo. For more information, please contact oadrcw.ls@ateneo.edu.



Non-tropical Cyclone Related Winter Heavy Rainfall Events over the Philippines: Climatology and Mechanisms

Lyndon Mark Olaguera^{1,2} · Jun Matsumoto^{1,3} · Julie Mae B. Dado² · Gemma Teresa T. Narisma^{2,4}

Received: 6 August 2019 / Revised: 30 October 2019 / Accepted: 25 November 2019 / Published online: 2 January 2020
© The Author(s) 2020, corrected publication 2020

Abstract

This study investigates non-tropical cyclone (TC) related boreal winter heavy rainfall events that lead to extensive flooding (HRF) over the Philippines through a case study and composite analysis. The HRF event examined occurred during January 16–22, 2017 over Cagayan de Oro City (CDO) in Mindanao Island (122–127°E, 5–10°N). The accumulated rainfall over CDO reached by about 180 mm from 00 UTC January 16 to 00 UTC January 17, 2017, exceeding the climatological maximum daily rainfall in January over this area. The interaction of a westward propagating cyclonic circulation over Mindanao Island (MCC) and a shearline that is associated with an eastward-propagating cyclonic and anticyclonic circulations along 20–40°N, led to enhanced moisture convergence and rainfall over CDO. The climatology of these non-TC related HRF events was examined through composite analysis of the HRF events documented in the Dartmouth Flood Observatory archive from 1979 to 2017. The authors identified 34 of such cases over the Philippines, in which 25 occurred over Mindanao Island. The composites of the circulation features of these 25 cases resemble those during the January 2017 case. A vorticity budget analysis was performed to explain the propagation tendency of the MCC. The results show that the MCC only propagated westward when the magnitudes of the stretching and advection terms of the vorticity tendency equation are almost comparable with each other, together with the weakening of the southerly winds around Mindanao Island. This study reveals how cold fronts over the north Pacific together with the MCC induces HRF events over the Philippines.

Keywords Philippines · Mindanao Island · Tail-end of a cold front · Winter monsoon · Vorticity budget

1 Introduction

Heavy rainfall/flood (HRF) events associated with synoptic-scale systems (i.e., systems that last for about 2–10 days) have profound agricultural and socio-economic impacts. Projections from multiple climate models used in the recent

assessment report by the Intergovernmental Panel on Climate Change (Stocker et al. 2013) show that the HRF events over the tropical regions are “very likely” to increase in the late twenty-first century. Located over the western rim of the Pacific Ocean, the Philippines (Fig. 1) is one of the countries over tropical Southeast Asia that is vulnerable to extreme HRF

Electronic supplementary material The online version of this article (<https://doi.org/10.1007/s13143-019-00165-2>) contains supplementary material, which is available to authorized users.

Responsible Editor: Edvin Aldrian.

✉ Lyndon Mark Olaguera
lyndonmarkolaguera@ed.tmu.ac.jp; lmolaguera@observatory.ph

Jun Matsumoto
jun@tmu.ac.jp

Julie Mae B. Dado
jimbado@observatory.ph

Gemma Teresa T. Narisma
gnarisma@ateneo.edu

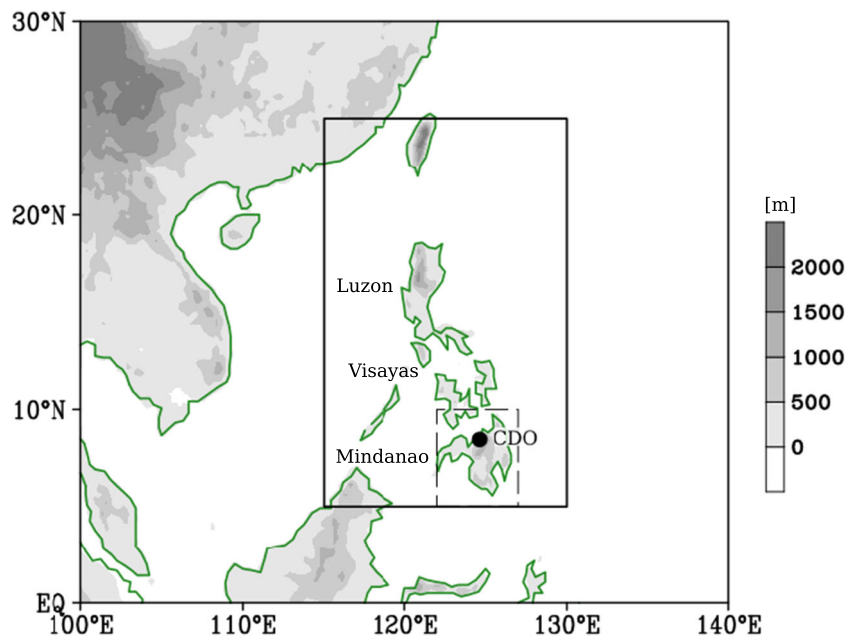
¹ Department of Geography, Tokyo Metropolitan University, 1-1 Minami-Osawa, Hachioji-Shi, Tokyo 192-0397, Japan

² Present address: Regional Climate Systems Laboratory, Manila Observatory, Ateneo de Manila University Campus, Loyola Heights, 1108 Quezon City, Philippines

³ Dynamic Coupling of Ocean-Atmosphere-Land Research Program, Japan Agency for Marine Earth Science and Technology, Yokosuka, Kanagawa 237-0061, Japan

⁴ Physics Department, Ateneo de Manila University, Loyola Heights, 1108 Quezon City, Philippines

Fig. 1 The topography (shades; m) of the Philippines and its three major island groups: Luzon, Visayas, and Mindanao (dashed box; 122–127°E, 5–10°N). The solid box (115–130°E, 5–25°N) indicates the domain used for removing the tropical cyclone influence in the study. The black circle indicates the location of Cagayan de Oro city (CDO)



events. Recent observational studies over the country show increasing trends in extreme rainfall (Cinco et al. 2014; Villafuerte II et al. 2014, 2015). Therefore, understanding the mechanisms leading to these HRF events is crucial for disaster management and mitigation.

HRF events over the Philippines occur almost throughout the year. Tropical cyclones (TC) generated over the South China Sea (SCS) and the Pacific Ocean are the primary cause of HRF events in the country, especially during the boreal summer monsoon season (Cayanan et al. 2011; Kubota et al. 2017). Aside from the rainfall brought by TCs upon landfall, it has been shown that non-landfalling TCs can also enhance the prevailing summer monsoon westerlies that bring more rainfall over the country (Cayanan et al. 2011). Nevertheless, the number of landfalling and non-landfalling TCs decreases in the succeeding boreal winter monsoon season (i.e., November to March), with the lowest number around March (Cinco et al. 2016). Hence, not all HRF events are associated with TCs. Such seasonality in the TC influence is related to the seasonal migration of the monsoon trough, which provides ambient condition for TC activity.

The HRF events during winter over the tropical Southeast Asia are often associated with cold surges (Yokoi and Matsumoto 2008; Faustino-Eslava et al. 2011), westward propagating cold surge vortices (CSVs) that is formed from the interaction of the cold surges and easterly waves (Chen et al. 2012, 2013, 2015a, b), and other sub-seasonal variabilities (Pullen et al. 2015; Takahashi et al. 2011). Yokoi and Matsumoto (2008) found that the interaction of cold surges and the westward propagating tropical depression (TD)-type disturbances (TDDs) is important for the formation of winter

HRF events over Vietnam and that the former, alone, does not contribute much to the total rainfall. Chen et al. (2012, 2013, 2015a, b) extensively examined the formation mechanism of westward propagating CSVs that induce HRF events over the Philippines, Vietnam, Peninsular Malaysia, and Borneo. They documented two types of CSVs: (1) the Philippine CSV that develops east of the Philippines due to the interaction of cold surge flow and easterly wave and the presence of an island-chain trough, and (2) the Borneo CSV that develops due to the interaction of the SCS cold surge flow, the near equatorial trough, and Borneo's orography. Chen et al. (2015b) noted that the average life cycle of CSVs from its formation time to the occurrence of the HRF event over the Philippines is about 1–4 days.

Frequent non-TC related HRF events during winter often cause heavy flooding over the Philippines. Pullen et al. (2015), for example, examined an HRF event during February 2008 and linked this event to the interaction of multi-scale systems such as the Indian Ocean Dipole, the strong La Niña condition, the coincidence with the Madden Julian Oscillation (MJO), and cold surge activity. Faustino-Eslava et al. (2011) and Yumul et al. (2013) also documented an HRF event over the Mindanao Island in the southern Philippines on January 2009, which they associated with a "tail end of a cold front". According to Yumul et al. (2013), the accumulated rainfall during January 2009 over Cagayan de Oro City (CDO; black circle in Fig. 1) of 300–400 mm is almost four times than its climatological rainfall value, which is 50–100 mm. Similar HRF events were reported in other parts of Mindanao Island during January 2009 that led to extensive flooding and multiple landslides. Another HRF

event occurred on January 2017 over Mindanao Island, which has been locally associated with the interaction of the “tail end of a cold front” and a Low-Pressure Area (LPA) by the Philippine Atmospheric Geophysical and Astronomical Services Administration (PAGASA), the country’s official weather bureau. Henceforth, this event will be referred to as JAN2017 HRF for brevity. This HRF event is discussed further in Section 3. The “tail end of a cold front” refers to the trailing end of an eastward propagating cold front in the north Pacific and is characterized by the interaction of the cold northeasterly winds and the warm easterly winds from the Pacific. Moreover, the JAN2017 HRF event is one of the extreme events recorded in the world in the year 2017 (Hoell et al. 2019; Christidis et al. 2019). This HRF event occurred briefly with no river overflow. While the urban flooding over CDO might be due to other factors that include infrastructure deficiencies (e.g., Japan International Cooperation Agency report, 2018), it is important to note that the climatological daily maximum rainfall for January is 31.1 mm day^{-1} from 1977 to 2013 at Lumbia Station (124.56°E , 8.40°N ; weather station of PAGASA) in CDO and this is sextupled in just one day (188.2 mm; weather station at SM City (124.62°E , 8.46°N) of the Weather Philippines Foundation Incorporated). We checked the ranks of the daily maximum rainfall in January from 1977 to 2013 at Lumbia Station in CDO and found that the JAN2017 HRF ranks first (not shown). Hence, choosing this HRF event as a case study seems practical. In order to improve the forecast of this HRF event, understanding the mechanisms inducing this event is necessary.

Several issues arise based on the documented winter HRF events over the Philippines:

- (1) Non-TC related HRF events such as cold surges also cause disastrous flooding over the Philippines. However, most of the previous studies only examined specific cases (e.g., Pullen et al. 2015) or focus on the impacts of these HRF events (e.g., Faustino-Eslava et al. 2011). How these non-TC related HRF events affect the country in the climatological mean sense have yet to be described in detail;
- (2) As will be shown later, the winter HRF events over the country occur more frequently over Mindanao Island (south of 10°N) from December to March of the succeeding year. This seems to be consistent with seasonal change in rainfall and winds over the country. The winter monsoon of the Philippines usually occurs from November to March and rainfall over the eastern coast gradually increases from north to south (Chen et al. 2015a; Kubota et al. 2017), concurrent with the seasonal change in the prevailing summer monsoon southwest-erlies to northeasterlies. While many studies have examined the rainfall variability in other parts of the Philippines such as Cruz et al. (2013) and Olaguera et al. (2018), the rainfall variability over Mindanao Island is less emphasized in these works. According to the recent agricultural statistics by the Philippine Statistics Authority (PSA) for the year 2017, a large portion of total corn (50%) and coconut (60%) productions came from Mindanao Island, indicating that it is an important agricultural region; therefore, understanding the rainfall variability over this region has important ramifications on the economy of the country;

The objectives of this study are therefore to examine the JAN2017 HRF event in detail and the climatology of non-TC related winter HRF events over Mindanao Island. The rest of the paper is organized as follows. Section 2 describes the various data sources and methodology used in this study. We investigated the recent extreme HRF during January 2017 and performed composite analyses to confirm the mechanisms in Sections 3 and 4, respectively. Section 5 presents the summary and discussion.

2 Data Sources and Methodology

2.1 Data Sources

This study utilized the following data sets:

- (1) Surface weather charts provided by the Japan Meteorological Agency (JMA) and archived by the National Institute of Informatics “Digital Typhoon” from 1979 to 2017 (<http://agora.ex.nii.ac.jp>).
- (2) Global heavy rainfall/flood (HRF) events compiled by the Dartmouth Flood Observatory (DFO) from 1979 to 2017 (<http://floodobservatory.colorado.edu>).
- (3) 6-hourly mean sea level pressure (*MSLP*), zonal (*U*) and meridional (*V*) wind components, relative humidity, and air temperature at multiple levels from the National Centers for Environmental Prediction-Department of Energy (NCEP-DOE) Atmospheric Model Intercomparison Project (AMIP-II), with $2.5^\circ \times 2.5^\circ$ horizontal grid resolution, from 1979 to 2017 (<https://www.esrl.noaa.gov/psd>; Kanamitsu et al. 2002).
- (4) 6-hourly TC best track archive from the Joint Typhoon Warning Center (JTWC; https://www.usno.navy.mil/NOOC/nmfc-ph/RSS/jtwc/best_tracks/wpindex.php) from 1979 to 2017.
- (5) 3-hourly rainfall from the Tropical Rainfall Measuring Mission (TRMM; https://disc.gsfc.nasa.gov/datasets/TRMM_3B42_V7/summary) 3B42RT version 7 with $0.25^\circ \times 0.25^\circ$ horizontal grid resolution, from January 15–16, 2017 (Huffman et al. 2010).



2.2 Methodology

First, we examined the large-scale circulation features during the JAN2017 HRF event over Mindanao Island using the JMA surface weather charts, TRMM rainfall, and winds at 925 hPa ($WINDS_{925hPa}$) including its components (i.e., U_{925hPa} and V_{925hPa}) from the NCEP-DOE reanalysis data set. The TRMM rainfall was converted to 6-hourly intervals to match the reanalysis data set. For example, the rainfall depicted at 06 UTC January 15 is the average rainfall from 03 to 06 UTC of January 15. We define Mindanao Island and its vicinity as the region within 122–127.5°E and 5–10°N (dashed box in Fig. 1), which for brevity, is simply referred to as “Mindanao Island”. This domain was defined to enclose the main island of Mindanao but not including other smaller islands of the region. As previously noted, the JAN2017 HRF event is associated with the interaction of the northeasterlies at the trailing end of an eastward propagating cold front and the prevailing easterlies. A confluence zone is established around Mindanao Island. This confluence zone is part of a deformation zone (i.e., total deformation, $TDef$), which can be mathematically represented by the combination of the stretching (STD) and shearing (SHD) deformations. In addition, to depict the mean position of the cold front from the reanalysis data set, we also analyzed the meridional gradient of the equivalent potential temperature at 925 hPa (θe_{925hPa}). These atmospheric parameters are further described in Section 3.

For the climatological analysis, we only selected HRF events not categorized as TC-related in the DFO archive and cases without TCs in the vicinity of the Philippines (115–130°E, 5–25°N; solid box in Fig. 1) from 1979 to 2017 using the JTWC TC best track data. This domain is similar to the Philippine Area of Responsibility (PAR; <http://bagong.pagasa.dost.gov.ph/learning-tools/philippine-area-of-responsibility>) by PAGASA with the eastern boundary 5° closer to the Philippines and the western and northern boundaries fixed at 115°E and 25°N, respectively. PAGASA only issues TC warnings for the country once the TC is within PAR. The western boundary of this domain covers the SCS since TCs located over this region can still enhance the prevailing northeasterly winds. We used the vertically integrated water vapor flux convergence as a proxy for rainfall for the climatological analysis since there are no available rainfall data sets with high spatio-temporal resolutions prior to 1997/1998. In addition, we analyzed the anomaly fields of the different atmospheric parameters for the climatological analysis. All anomalies are relative to the 1981–2010 mean.

3 Large-Scale Circulation Features during the JAN2017 HRF Event

In this section, we examine the large-scale circulation features during the JAN2017 HRF event. An extreme flooding over CDO (124.63°E, 8.45°N) was reported around the afternoon of January 16, 2017 (between 06 and 12UTC). A weather station by the Weather Philippines Foundation Incorporated, located over CDO recorded a 24-h accumulated rainfall of about 188.20 mm from 00 UTC January 16, 2017 to 00 UTC January 17, 2017 (<https://weather.ph.org/understanding-the-weather-conditions-behind-the-cagayan-de-oro-flooding>). The horizontal wind field at 925 hPa ($WINDS_{925hPa}$) during 06 UTC January 16, 2017 (Fig. 2a) features cyclonic circulations over Mindanao Island and in the broad North Pacific along 20–50°N centered around 45°N, 180°. It is worth mentioning that cold fronts are usually depicted at 925 hPa level (e.g., Utsumi et al. 2014) and since the JAN2017 HRF event is associated with a frontal system, we used this pressure level to illustrate the large-scale circulation features throughout the manuscript. Nevertheless, we confirmed that similar circulation features can be depicted at 850 hPa level. The magnitude of the $WINDS_{925hPa}$ over the central and northern Philippines is about 10 m s^{-1} , which is almost twice the climatological wind speed (5 m s^{-1} ; Fig. 2b) in these regions. Such enhanced $WINDS_{925hPa}$ during the JAN2017 HRF event might be due to the enhanced pressure gradient induced by the cyclonic circulation around Mindanao Island and the anticyclonic circulation to its north. The zonal wind anomaly at 925 hPa (U_{925hPa} ; Fig. 2c) features enhanced westerlies over Mindanao Island and enhanced easterlies over the central and northern Philippines. On the other hand, the meridional wind anomaly (V_{925hPa} ; Fig. 2d), shows enhanced northerlies penetrating over northern Borneo and enhanced southerlies over Mindanao Island. The enhanced westerly and southerly wind anomalies over Mindanao Island might have brought more moisture, resulting in heavier rainfall.

Figure 3 shows the synoptic charts from 06 UTC January 15, 2017 to 12 UTC January 16, 2017. Some remarkable features at 06 UTC January 15, 2017 (Fig. 3a) include the TD located in the south of Vietnam, the LPA that is located in the east of Japan along 40°N, and the southeastern ridge of the anticyclonic circulation located in the north of Luzon Island. At 12 UTC January 15, 2017 and 18 UTC (Figs. 3b and c), the southeastern ridge of the anticyclonic circulation in the north of Luzon Island extends further southward and the LPA along 40°N further intensify. An LPA developed south of 10°N at 00 UTC January 16, 2017 (Fig. 3d) and briefly intensified around 06 UTC (Fig. 3e). Note also that the center of the LPA over Mindanao Island, which is denoted as “L”, moved slightly westward (Figs. 3d to e). At 12 UTC January 16, 2017 (Fig. 3f), this LPA weakens.

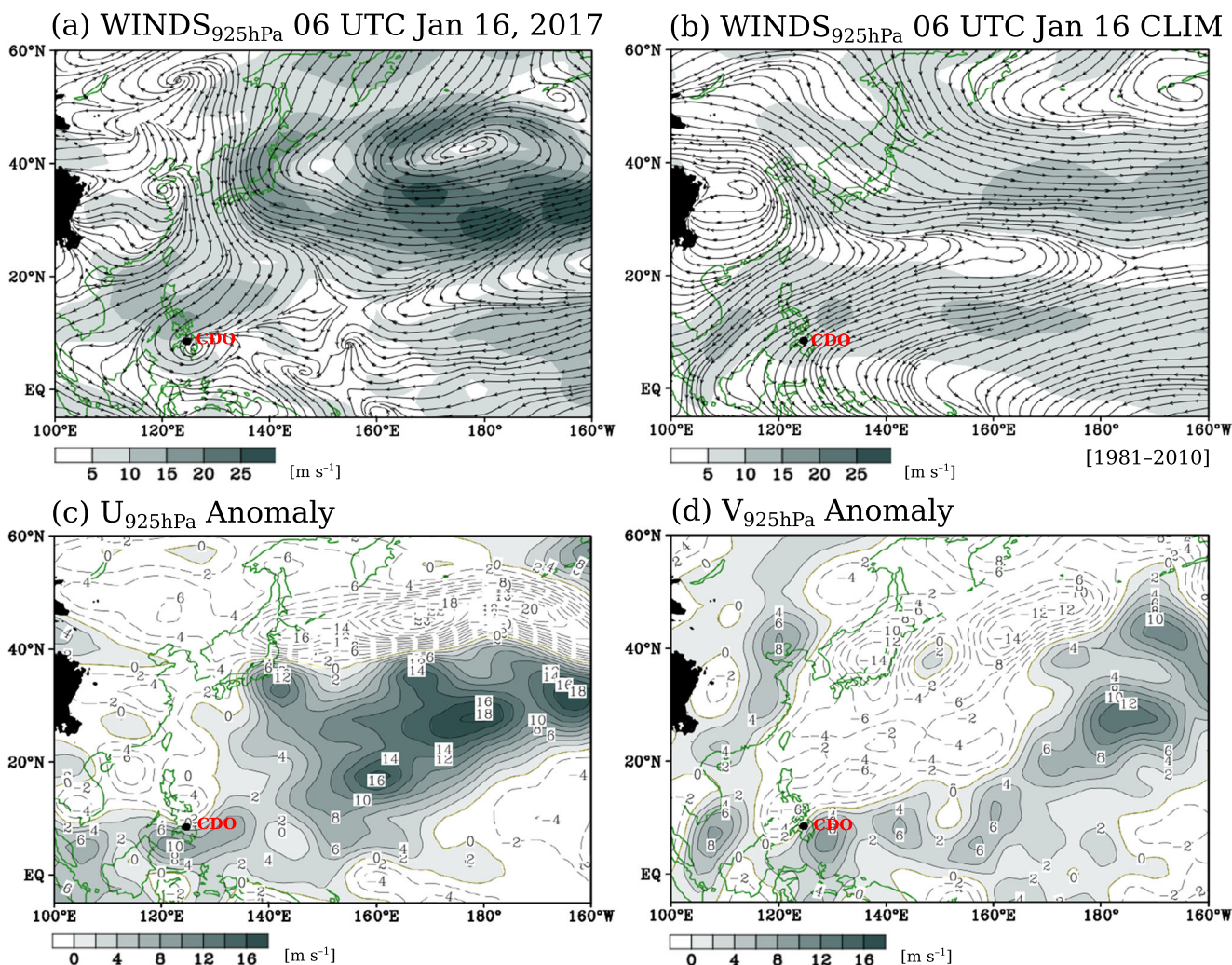


Fig. 2 Horizontal winds at 925 hPa ($WINDS_{925hPa}$; shades and contours; $m s^{-1}$) on: (a) 06 UTC January 16, 2017; and (b) its corresponding climatology (06 UTC January 16; 1981–2010). Anomalies of the 925 hPa: (c) zonal (U_{925hPa} ; shades and contours; $m s^{-1}$); and (d)

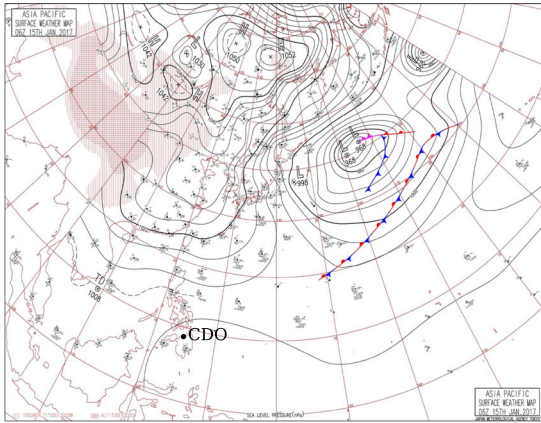
meridional (V_{925hPa} ; shades and contours; $m s^{-1}$) winds. Shadings in (a) and (b) indicate the magnitude of the $WINDS_{925hPa}$. The contour interval in (c) and (d) is $2 m s^{-1}$. The black circle indicates the location of Cagayan de Oro City (CDO)

As we have mentioned previously, the JAN2017 HRF event was associated with the “tail-end of a cold front” and its interaction with the LPA over Mindanao Island, as denoted by PAGASA. However, in Fig. 3, this cold front is located to the east of the Philippines (east of $160^{\circ}E$) and may not be directly interacting with the LPA over Mindanao Island. Hence, associating this with the “tail-end of a cold front” needs further clarification.

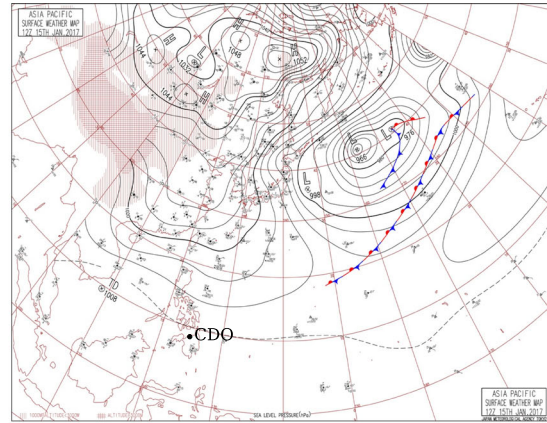
Figure 4 shows the TRMM rainfall superimposed with the $WINDS_{925hPa}$ from 06 UTC January 15, 2017 to 12 UTC January 16, 2017. There are two anticyclonic circulations centered around $120^{\circ}E, 35^{\circ}N$ (A_1) and $140^{\circ}W, 30^{\circ}N$ (A_2) that are juxtaposed in a northwest-southeast orientation (NW-SE; a similar abbreviation method will be used in the succeeding sections) at 06 UTC January 15, 2017 (Fig. 4a). In the same figure, two cyclonic circulations centered around $165^{\circ}E, 40^{\circ}N$ (C_1) and $125^{\circ}E, 8^{\circ}N$ (C_2) are also juxtaposed in a SW-NE

orientation. In addition, another cyclonic circulation can also be depicted in the south of Vietnam (around $10^{\circ}N$; Fig. 4a), which is associated with the TD in the synoptic charts in Fig. 3a. Note that at 06 UTC January 16, 2017, the TD has already weakened (Figs. 3e and 4e). In addition, this TD is no longer clear at 925 hPa from 18 UTC January 15, 2017 to 00 UTC January 16, 2017, as shown in Figs. 4c and d, although it is still indicated in the surface weather charts until 00 UTC January 16, 2017 (Figs. 3c and d). This indicates that this dissipating TD is only detectable near the surface level. The northeasterlies from A_1 interact with the easterlies of the TD and C_2 , while the southwesterlies on the western flank of A_2 interact with the northwesterlies on the western flank of C_1 . The northeasterlies from A_1 bring cool air from the mid-latitudes, while the easterlies from C_2 bring warm and humid air from the tropics. The interaction of these two systems forms a confluence region, which is known as a *shearline* (e.g.,

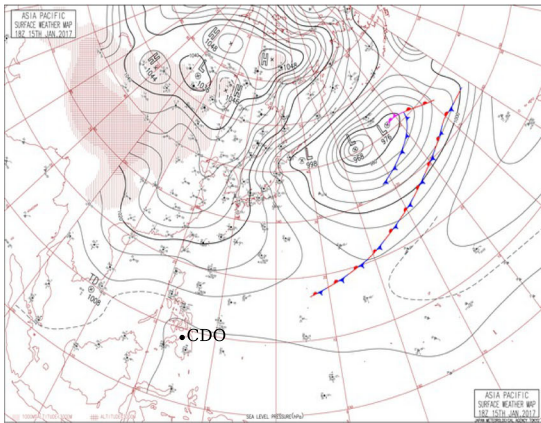
(a) 06 UTC Jan 15, 2017



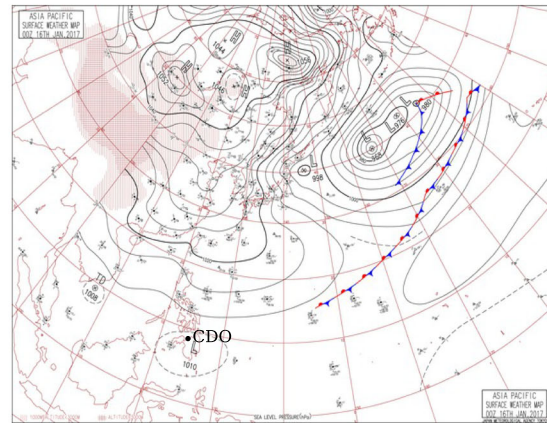
(b) 12 UTC Jan 15, 2017



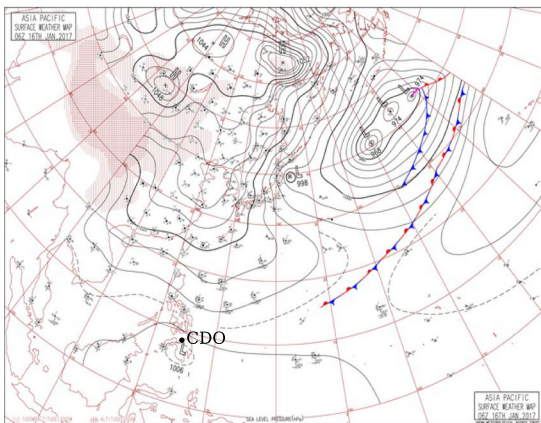
(c) 18 UTC Jan 15, 2017



(d) 00 UTC Jan 16, 2017



(e) 06 UTC Jan 16, 2017



(f) 12 UTC Jan 16, 2017

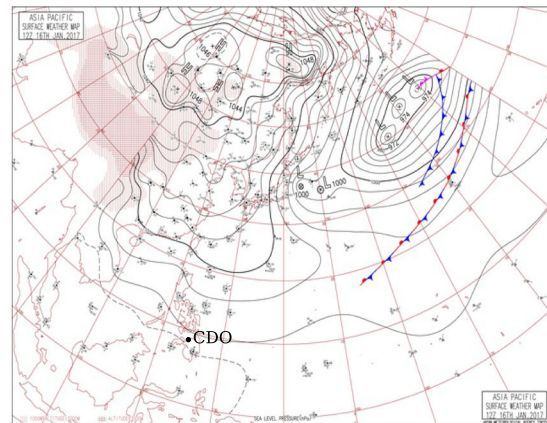


Fig. 3 Surface weather charts provided by the Japan Meteorological Agency for: (a) 06 UTC January 15, 2017; (b) 12 UTC January 15, 2017; (c) 18 UTC January 15, 2017; (d) 00 UTC January 16, 2017; (e)

06 UTC January 16, 2017; and (f) 12 UTC January 16, 2017. The black dot indicates the location of Cagayan de Oro City (CDO)

Cabanerit 2016). In general, the shearline is just part of a deformation zone and lies along its axis of dilatation. The total deformation ($TDef$) can be represented, mathematically, as the sum of the stretching (STD) and shearing (SHD) deformations ([http://www.zamg.ac.at/docu/Manual/SatManu/main.htm/](http://www.zamg.ac.at/docu/Manual/SatManu/main.htm?/)

<http://www.zamg.ac.at/docu/Manual/SatManu/CMs/Def/backgr.htm>). These are calculated as follows:

$$STD = \frac{\partial U}{\partial x} - \frac{\partial V}{\partial y}, \quad (1)$$

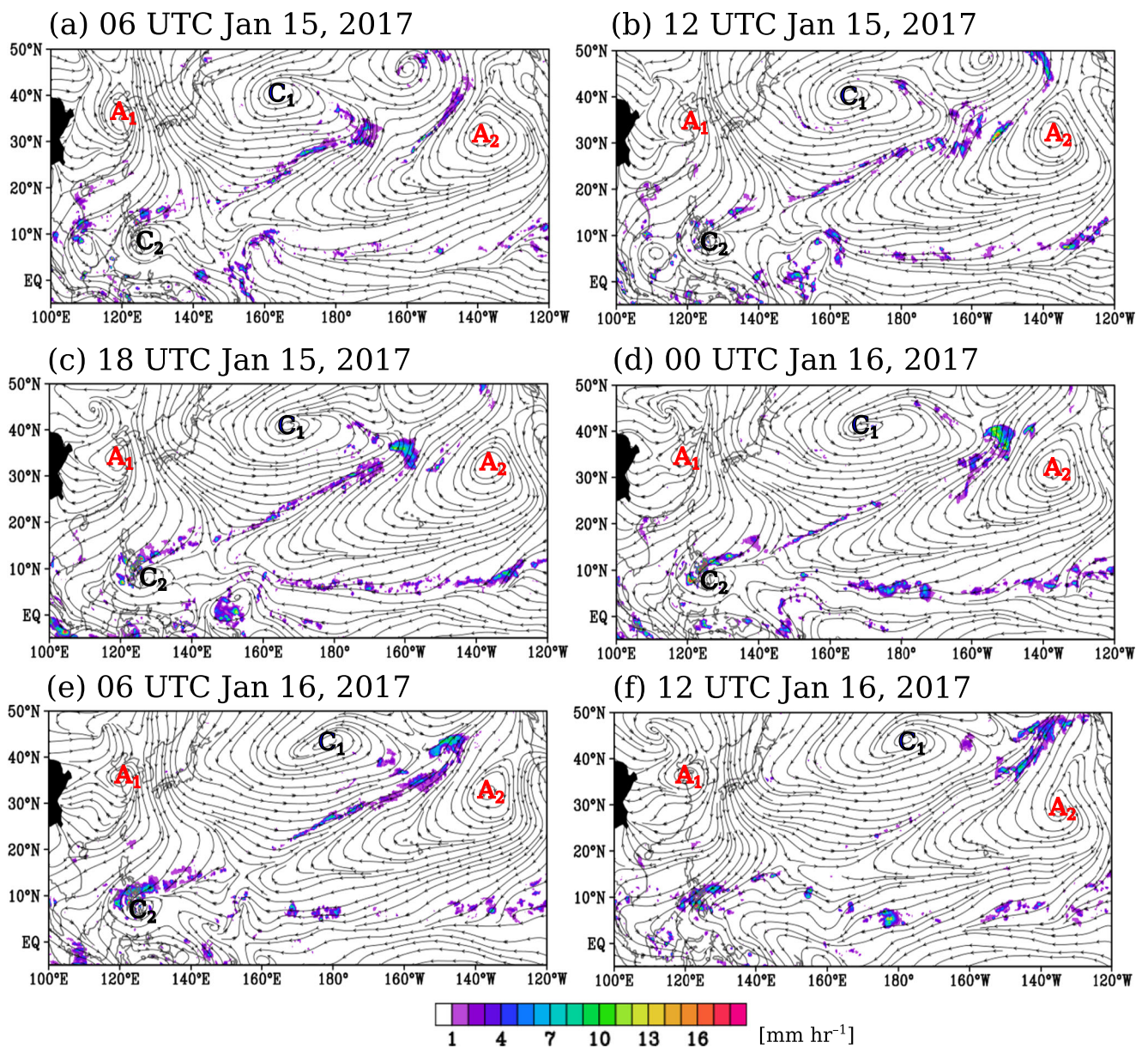


Fig. 4 As in Fig. 3 but for the distribution of rainfall from the Tropical Rainfall Measuring Mission (TRMM) 3B42 version 7 (shades; mm hr⁻¹) and 925 hPa winds ($WINDS_{925hPa}$; streams; m s⁻¹). The cyclonic and anticyclonic circulations are denoted as “C” and “A”, respectively

$$SHD = \frac{\partial U}{\partial y} + \frac{\partial V}{\partial x}, \tag{2}$$

$$TDef = \sqrt{STD^2 + SHD^2}, \tag{3}$$

where U and V are the zonal and meridional wind components, respectively. We illustrate the STD_{925hPa} , SHD_{925hPa} , and $TDef_{925hPa}$ in Fig. 5 to show the location of the shearline at 06 UTC January 16, 2017. Also shown is the meridional gradient of θe_{925hPa} to indicate the mean position of the cold front. During this period, the location of the deformation zone is centered around 155°E, 15°N, as indicated by the star in

Fig. 5. The southern edge of A_1 extends further south of 10°N. The cold front is oriented in a southwest-northeast direction from 120°E to 120°W just to the north of the deformation zone (Fig. 5a). The shearline coincides with the region of more positive STD_{925hPa} , indicating that the horizontal wind gradient/shear (i.e., $\partial U_{925hPa}/\partial x$) is large along this region (Fig. 5b). On the other hand, the SHD_{925hPa} (Fig. 5c) is weaker on the western side of the deformation zone but stronger on the eastern side. This suggests that the STD_{925hPa} is more important in inducing the JAN2017 HRF event and that it contributed more to the $TDef_{925hPa}$, as shown in Fig. 5d. Along the shearline, cold air from A_1 and warm air over the

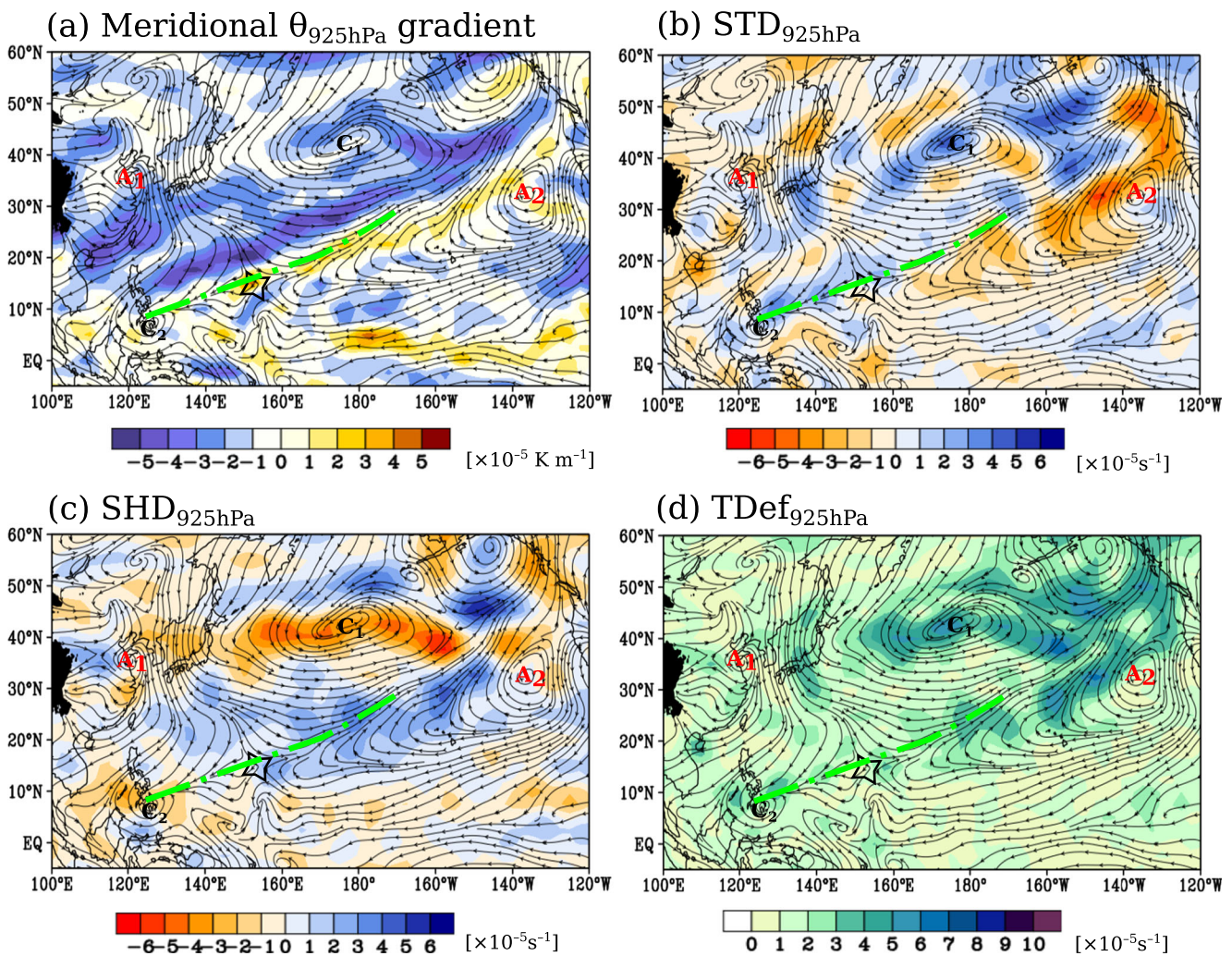


Fig. 5 Spatial distribution of the 925 hPa: (a) meridional equivalent potential temperature gradient ($\theta_{e925hPa}$; shades; $\times 10^{-5} \text{ K s}^{-1}$); (b) stretching deformation (STD_{925hPa} ; shades; $\times 10^{-5} \text{ s}^{-1}$); (c) shearing deformation (SHD_{925hPa} ; shades; $\times 10^{-5} \text{ s}^{-1}$); and (d) total deformation ($TDef_{925hPa}$; shades; $\times 10^{-5} \text{ s}^{-1}$) at 06 UTC January 16, 2017. The

925 hPa wind anomalies (streams; m s^{-1}) are superimposed for discussion. The black star indicates the location of the deformation zone. The “A” and “C” are similar to those in Fig. 4. The dot-dashed green line indicates the location of the shearline

tropics induces enhanced convergence over Mindanao Island, as will be shown later. We also found enhanced mid-tropospheric ascent over the same region since warm air is pushed upwards by the cooler air (not shown).

The rainfall distribution from the TRMM data, as shown in Fig. 4, depicts a SW-NE oriented band of rainfall from the SCS to the north Pacific along the shearline. At 06 and 12 UTC January 15, 2017 (Figs. 4a and b, respectively), this rainfall band is located north of 10°N and rainfall clusters can only be depicted over the central Philippines. At 18 UTC January 15, 2017 and 00 UTC January 16, 2017 (Figs. 4c and d, respectively), this rainfall band progresses southward, concurrent with the weakening of the TD in the south of Vietnam. At 06 and 12 UTC January 16, 2017 (Figs. 4e and f, respectively), the rainfall clusters over Mindanao Island become well defined, especially along the shearline.

Although, no more cyclonic circulation change can be depicted over Mindanao Island, a trough still exists in the same region.

3.1 Maintenance of the JAN2017 HRF Event

Rainfall is maintained by the convergence of water vapor flux (Q ; Chen et al. 2013). According to Chen (1985), Q can be split into its rotational (Q_R) and divergent (Q_D) components:

$$Q = Q_R + Q_D, \quad (4)$$

where $Q = (1/g) \int_{p_{300}}^{p_{1000}} \mathbf{V} q dp$, g , \mathbf{V} , p , and q are the water vapor flux ($\text{kg m}^2 \text{ s}^{-1}$), gravitational constant (m s^{-2}), wind vector (m s^{-1}), pressure (mb), and specific humidity (g g^{-1}), respectively. The Q_R and Q_D , can also be expressed in terms of

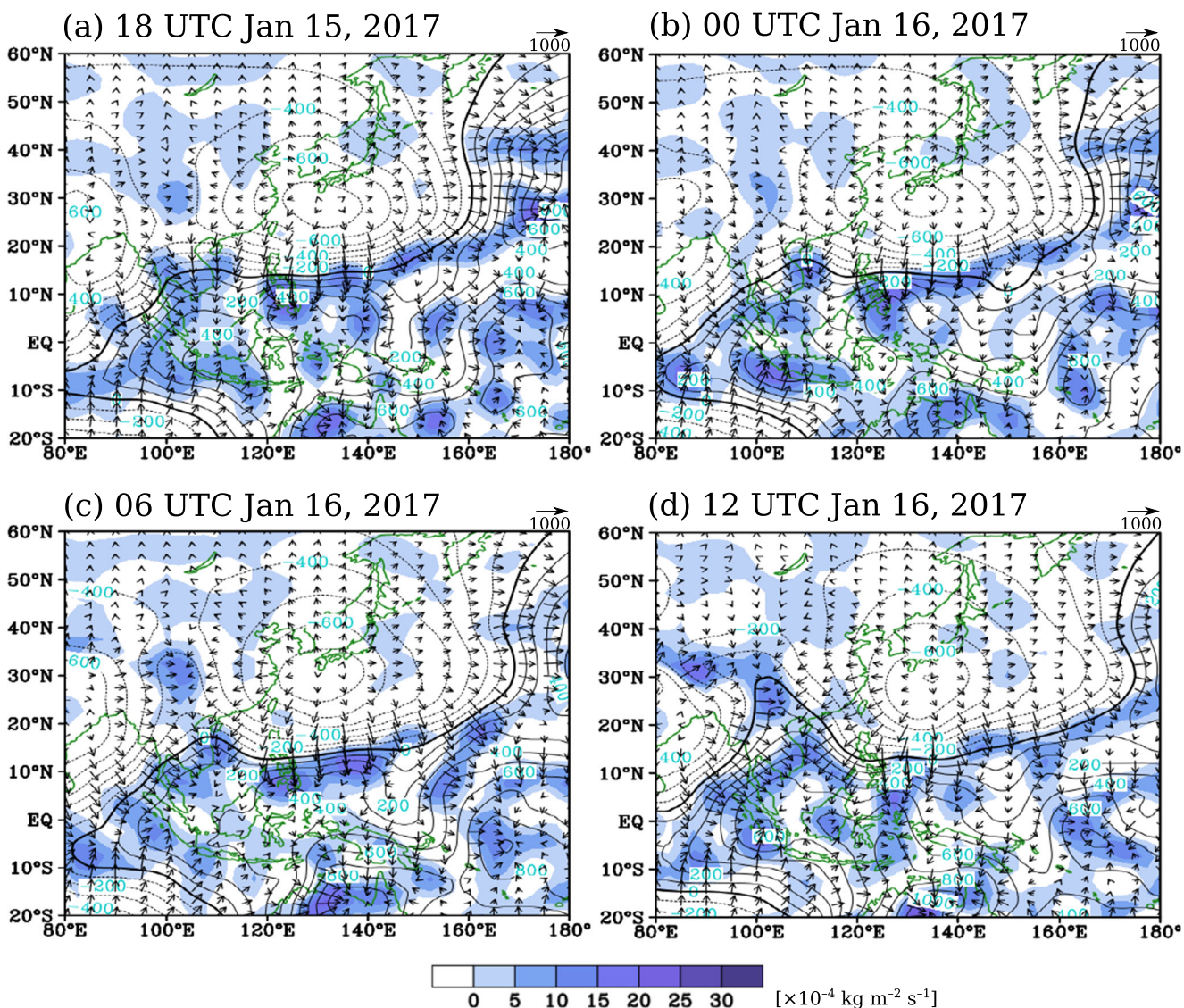


Fig. 6 Spatial distribution of vertically integrated moisture flux convergence (Q ; shades; $\times 10^{-4} \text{ kg m}^{-2} \text{ s}^{-1}$), velocity potential (χ_Q ; contours; $\times 10^6 \text{ kg s}^{-1}$), and the divergent component of Q (Q_D ; vectors; $\text{kg m}^{-1} \text{ s}^{-1}$) for: (a) 18 UTC January 15, 2017; (b) 00 UTC

January 16, 2017; (c) 06 UTC January 16, 2017; and (d) 12 UTC January 16, 2017. The contour interval of χ_Q is $100 \times 10^6 \text{ kg s}^{-1}$, while the scale of the vectors is $1000 \text{ kg m}^{-1} \text{ s}^{-1}$

the horizontal gradients of the streamfunction ($Q_R = \mathbf{k} \times \nabla \psi_Q$) and velocity potential ($Q_D = \nabla \chi_Q$), respectively. Thus, rainfall (P) can be approximated as:

$$P \approx \nabla \cdot Q_D = -\nabla^2 \chi_Q \tag{5}$$

The maintenance of rainfall is illustrated by the spatial plots of χ_Q , Q_D , and Q in Fig. 6, following Chen et al. (2013). A prominent north-south contrast of convergent and divergent fluxes during the JAN2017 HRF event can be seen over the tropical southeast Asia. The zero-contour line splits these two opposing circulations along 15°N over the Philippines. The enhanced Q can be seen in the downstream of the northerly

fluxes along this zero-contour line (Fig. 6a), which is consistent with the location of enhanced rainfall, as shown in Fig. 4. The divergent fluxes originate from the negative χ_Q center (130°E , 28°N) in the south of Japan, which is part of A_1 in Fig. 4. Northerly fluxes appear to be confined along 10°N at 18 UTC January 15, 2017 (Fig. 6a) and a convergence region is located downstream of these northerly fluxes in the eastern side of Mindanao Island. At 06 UTC January 16, 2017, this convergence region shifts westward (Figs. 6c and d), which is consistent with Fig. 4d and e. At 12 UTC January 16, 2017 (Fig. 6d), the northerly fluxes further intrude the equatorial region and the convergence region near Mindanao Island is located further south over the Indonesian archipelago.

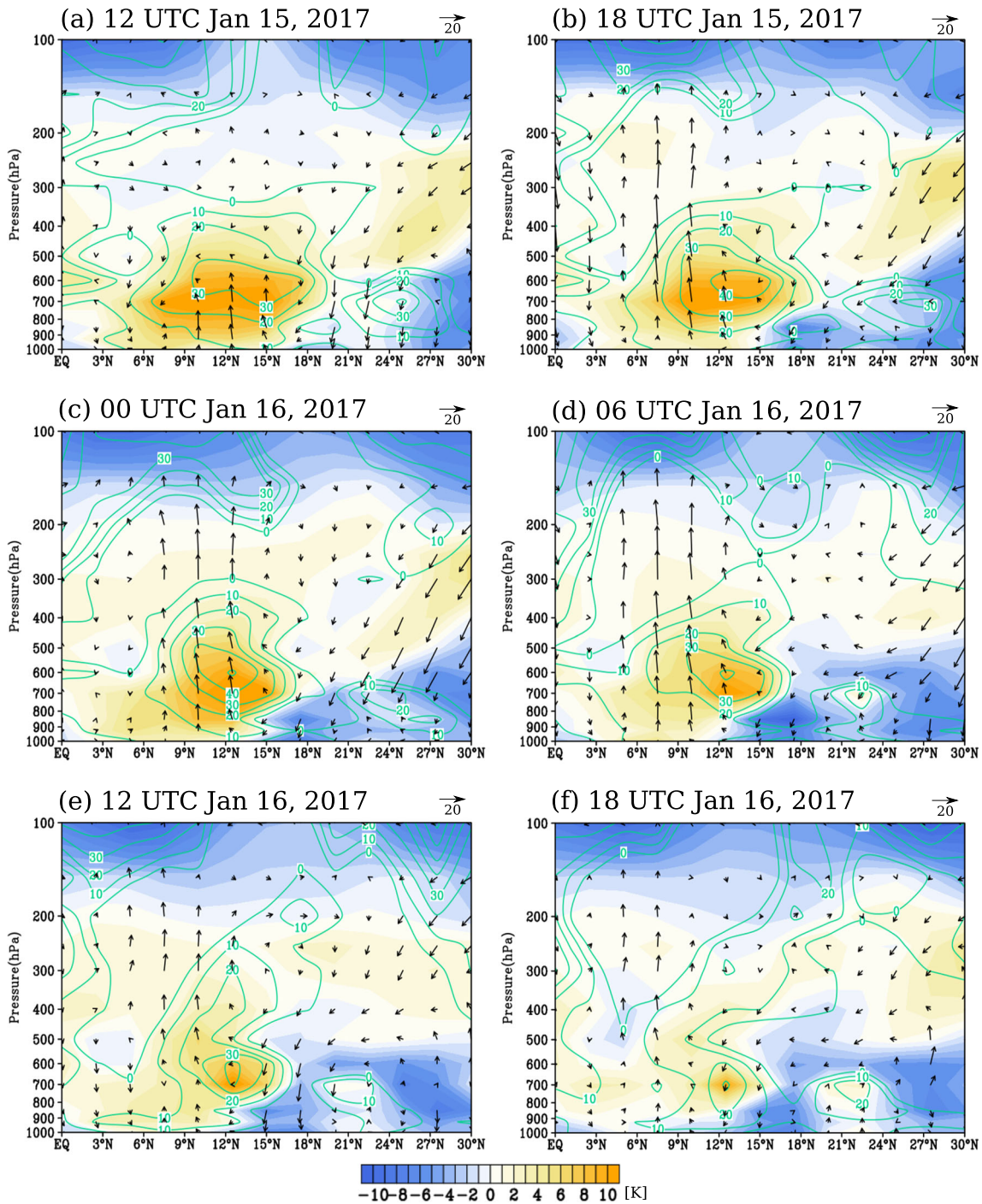


Fig. 7 Vertical profile of the equivalent potential temperature anomaly (shades; K) and relative humidity anomaly (contours; %) averaged from 122 to 127.5°E for: (a) 12 UTC January 15, 2017; (b) 18 UTC January 15, 2017; (c) 00 UTC January 16, 2017; (d) 06 UTC January 16, 2017; (e) 12

UTC January 16, 2017; and (f) 18 UTC January 16, 2017. The vectors are the meridional ($m s^{-1}$, scale is $20 m s^{-1}$) and vertical velocity anomalies (hPa , scale is $20 hPa$). The anomalies are relative to the 1981–2010 mean

3.2 The Vertical Structure of the Shearline

To further clarify the vertical structure of the shearline, we derived the pressure-latitude cross-section of the θ_e (shades) and relative humidity (%) anomalies averaged from 122

to 127.5°E, as shown in Fig. 7. At 12 UTC January 15, 2017 (Fig. 7a), the warm θ_e anomaly is slightly tilted with height to the north and the warmest region is located between 6 and 18°N, while the relative humidity anomaly appears to be standing below the 300 hPa level. The location of the warmest

θe anomaly coincides with the location of the maximum relative humidity anomaly. Ascending anomalies between these latitudes are confined below 600 hPa. From 18 UTC January 15, 2017 (Fig. 7b) to 00 UTC January 16, 2017 (Fig. 7c), the cold θe anomaly below 700 hPa expands to the south along 15°N and the ascending anomalies south of this latitude reach 200 hPa. Concurrently, the relative humidity anomaly also increases to about 40%. Also remarkable are the enhanced descending anomalies in the north of 18°N, indicating an enhanced cold surge activity. At 06 UTC January 16, 2017 (Fig. 7d), the warm θe anomaly weakens and the cold θe anomaly to its north penetrates 12°N. At 12 UTC January 16, 2017 (Fig. 7e), the ascending anomalies between 6 and 12°N weaken, which is consistent with the weakening of rainfall during this period. In addition, positive relative humidity anomaly starts to extend in the upper levels (i.e., 200 hPa). At 18 UTC January 16, 2017 (Fig. 7f), the cold θe anomaly below 900 hPa penetrates the equatorial region and the relative humidity anomaly decreases to about 20%. These changes are consistent with the northeasterly wind intrusion over the Philippines during this period.

In summary, we examined a non-TC related HRF event that occurred on January 2017 over Mindanao Island in the southern Philippines. This HRF event is induced by the interaction of an anomalous westward propagating cyclonic circulation over Mindanao Island and the shearline that is associated with an eastward propagating cyclonic and anticyclonic circulations over the north Pacific. We refer to this cyclonic anomaly over Mindanao Island as “MCC” for brevity. The MCC strengthened the prevailing northeasterlies in the lower troposphere, which favored the enhancement of moisture convergence and rainfall in the same region.

4 Climatology of Non-TC Related Winter HRF Events over Mindanao Island

Using the flood reports from the DFO, we checked all HRF events from 1979 to 2017 and validated them using the surface weather charts. We only considered those cases that were not categorized as TC-induced (i.e., those cases due to shearlines, etc.) and cases when there was no reported TC within 110–130°E and 5–25°N. There are 34 HRFs over the Philippines satisfying the above criteria, in which 25 cases (74%) occurred over Mindanao Island. Since most of the cases occurred over Mindanao Island, we focus our analysis over this region in the succeeding sections. We classified the HRFs per month as shown in Fig. 8. A majority of the cases occurred between December and March. This distribution appears to be consistent with the southward progression of the northeast monsoon over the Philippines (e.g., Kubota et al. 2017; Chen et al. 2015b). In particular, three cases occurred during

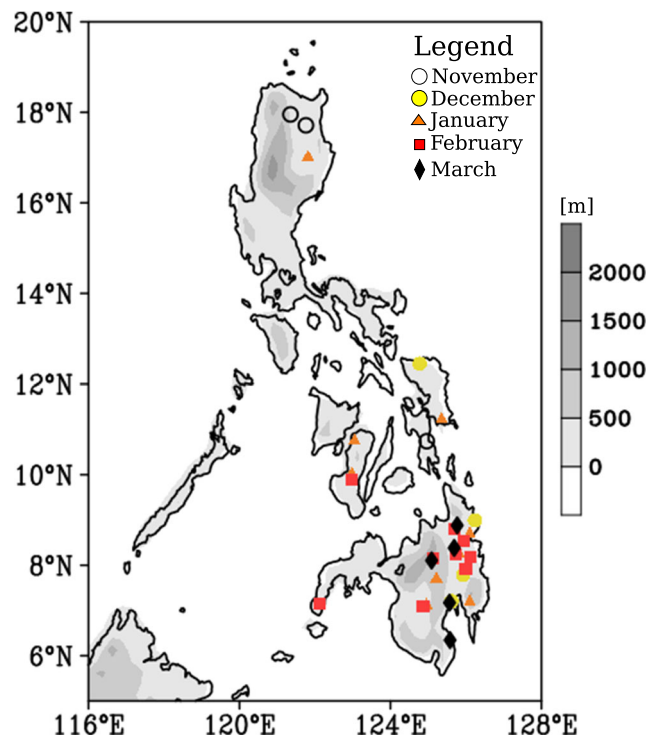


Fig. 8 The location of the 34 non-tropical cyclone related heavy rainfall/flood (HRF) events from November to March superimposed on the Philippine topography (shades; m) from 1979 to 2017 based on the Dartmouth Flood Observatory archive

December, eight cases during January, nine cases during February, and five cases during March in Mindanao Island.

Unfortunately, we do not have a homogenous rainfall data over this area and since we are interested in the climatology of non-TC related HRF events, we need an index to represent them. Note that in the JAN2017 HRF event, the region with enhanced rainfall coincides with the region of enhanced Q over Mindanao Island. Banacos and Schultz (2005) noted that Q can be used as a proxy for rainfall associated with synoptic-scale systems. Hence, in this study, we represented the HRF event using Q . The duration and the location of the HRF events are included in the DFO archive. We checked the time series of the Q in each of the 25 cases and defined Lag 0 as the time when the area-averaged Q over Mindanao Island of the reported HRF event attains its maximum value. Then, we performed lag-composites to determine the controlling mechanisms of these HRF events.

Figure 9 shows the lag composites of $WINDS_{925hPa}$ and $MSLP$ anomalies from Lag -3 to Lag +15. The significant $MSLP$ and $WINDS_{925hPa}$ anomalies are shown in Figure S1. A westward propagating cyclonic anomaly can be seen over Mindanao Island, while an eastward propagating cyclonic and an anticyclonic circulation behind it can be depicted along 20–40°N. Such circulation features resemble those from the JAN2017 HRF event, suggesting that they are common for the winter HRF events over

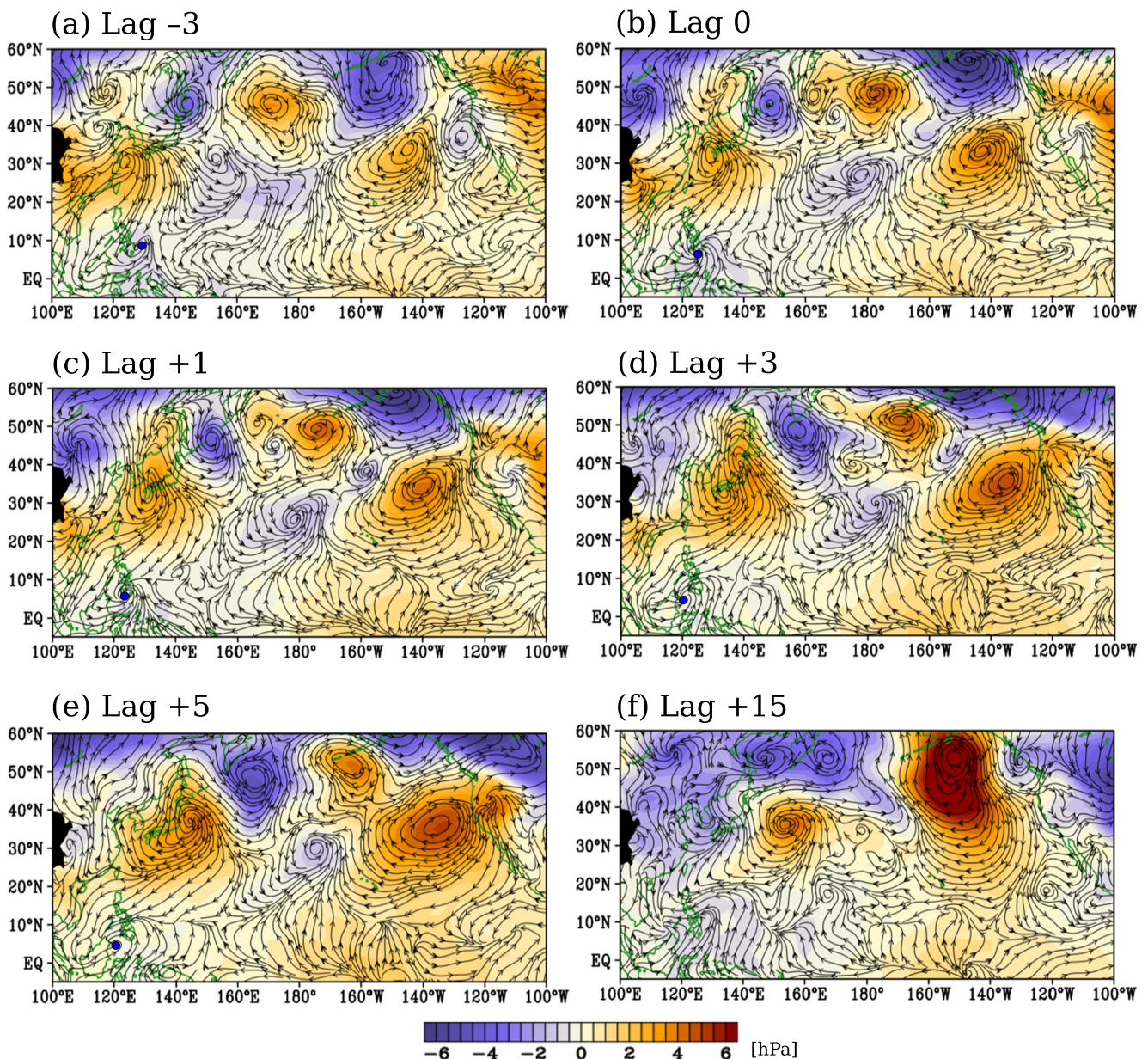


Fig. 9 Lag composite anomalies of mean sea level pressure (shades; hPa), 925 hPa winds (streams; m s^{-1}) for: (a) Lag -3; (b) Lag 0; (c) Lag +1; (d) Lag +3; (e) Lag +5; and (f) Lag +15. Lag 0 refers to the time when the area-averaged vertically integrated moisture flux convergence (VIMFC) of the recorded HRF event over Mindanao

Island is maximum. Note that the reanalysis data is 6-hourly so that Lag -3 (+3) means 18 h before (after) the peak VIMFC. The blue circle indicates the center of the anomalous cyclonic circulation over Mindanao Island (MCC)

Mindanao Island. At Lag -3 (Figure 9a), the MCC is located off the coast of Mindanao Island around 127°E , 5°N . At the same time, an anomalous anticyclone can be depicted around 122°E , 30°N and an anomalous cyclonic circulation can be depicted around 155°E , 30°N . Northeasterly $\text{WINDS}_{925\text{hPa}}$ are apparent over the Philippines. These northeasterly $\text{WINDS}_{925\text{hPa}}$ are significant over the north of 10°N over the Philippines (Figure S1a). A confluence region between the northeasterly $\text{WINDS}_{925\text{hPa}}$ and south/southeasterly $\text{WINDS}_{925\text{hPa}}$

from the MCC is located along 10°N . At Lag 0 (Figure 9b), the MCC is located over Mindanao Island. The significant $\text{WINDS}_{925\text{hPa}}$ anomalies covers the entire Philippines with significant anomalous cyclonic circulation over Mindanao Island (Figure S1b). Significant MSLP anomalies can also be found around Mindanao Island (Figure S1b). The anomalous anticyclonic and cyclonic circulation anomalies along $20\text{--}40^{\circ}\text{N}$, move eastward (Figure 9b). At Lag +1 (Figure 9c), the MCC shifts to the west of Mindanao Island around 122°E , 5°N .

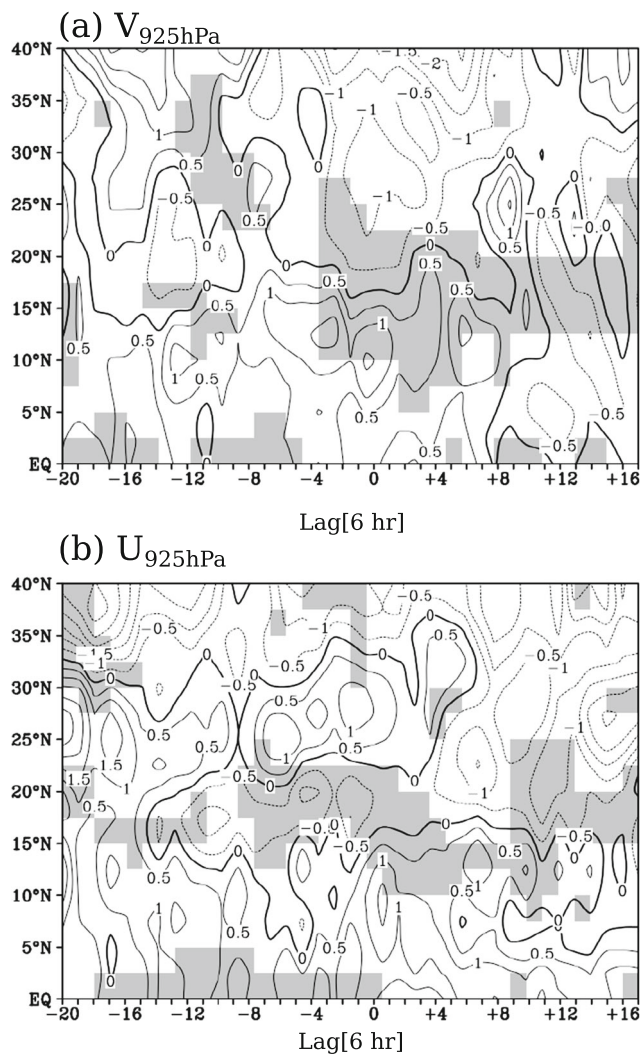


Fig. 10 Composite anomalies of: (a) 925 hPa meridional wind (V_{925hPa} ; shades and contours; $m s^{-1}$); and (b) 925 hPa zonal winds (U_{925hPa} ; shades and contours; $m s^{-1}$) averaged from 122 to 127.5°E. The contour interval is 0.5 $m s^{-1}$. The shaded areas indicate statistical significance at the 90 % confidence level using Student's t -test

Significant northeasterly $WINDS_{925hPa}$ anomalies begin to reach 5°N (Figure S1c). At Lag +3 (Figure 9d), the MCC is located around 120°E, 5°N. Significant easterly $WINDS_{925hPa}$ anomalies are now apparent over Mindanao Island. The anomalous anticyclone is located over Japan, while northeasterly $WINDS_{925hPa}$ affect the Philippines. At Lag +5 (Figure 9e), the MCC is no longer defined, while another anomalous cyclonic circulation develops to the west of Borneo. At the same time, significant easterly $WINDS_{925hPa}$ are apparent over the Philippines (Figure S1b). At Lag +15 (Figure 9f), easterly to southeasterly $WINDS_{925hPa}$ anomalies are apparent over the Philippines that is accompanied by positive MSLP anomaly. However, only the $WINDS_{925hPa}$ anomalies are significant over the country (Figure S1f).

4.1 Intensification and Westward Propagation of the MCC

Yokoi and Matsumoto (2008) examined a cold surge (CS) event during November 1999 over central Vietnam that lingered there for several days. They suggested that the strong southerly winds over the central SCS prevented this CS from propagating southwards. The MCC did not show southward propagation tendency from the composite anomalies. Therefore, we examine first the time-latitude cross section of the U_{925hPa} and V_{925hPa} in Fig. 10.

The time-latitude cross section of V_{925hPa} anomaly (Fig. 10a) shows enhanced southerly winds south of 15°N from Lag -20 to Lag +8. The southerly V_{925hPa} starts to intensify at Lag -5 between 10 and 15°N. Easterly U_{925hPa} appears along 5–10°N between Lag -7 and Lag -4 (Fig. 10b). At Lag 0, enhanced southerly V_{925hPa} appears along 5–10°N, which is concurrent with the intensification of westerly U_{925hPa} along the same latitude band. These changes favor the enhancement of the MCC. The southerly V_{925hPa} might have also facilitated the transport of warm and humid air from the equatorial region that interacted with the cool and dry northeasterlies. After Lag +1, the southerly V_{925hPa} weakens. These changes favor the southward/southwestward propagation of the MCC, as shown in Fig. 9. At Lag +8, northerly V_{925hPa} and easterly U_{925hPa} begin to penetrate the equatorial region concurrent with the westward propagation of the MCC.

On the other hand, Chen et al. (2015b) examined the westward propagating CS vortices (CSVs) during the winter monsoon season over the western North Pacific. They used vorticity budget analysis to diagnose the intensification and propagation tendencies of these CSVs. The vorticity tendency can be used to represent such propagation tendencies and can be calculated as follows:

$$\xi_t = -\mathbf{V} \cdot \nabla(\xi + f) - (\xi + f)\nabla \cdot \mathbf{V}, \tag{6}$$

where f is the Coriolis parameter (s^{-1}) and \mathbf{V} is the wind vector ($m s^{-1}$). The first term on the right-hand side of Equation 6 denotes the vorticity advection (ξ_{adv}), while the second term indicates the vorticity stretching ($\xi_{stretch}$). Chen et al. (2015b) noted that the westward propagation of CSVs is facilitated by a positive ξ_{adv} to the west of the central vortex and larger values of ξ_{adv} compared with the $\xi_{stretch}$.

Figures 11 and 12 show the ξ_t , ξ_{adv} , $\xi_{stretch}$ anomalies superimposed with the $WINDS_{925hPa}$ anomalies to depict the location of the MCC. At Lag -3 (Fig. 11a to c), the spatial distribution of ξ_{adv} (Fig. 11b) shows favorable conditions (i.e., positive ξ_{adv} to the west of the vortex center) for westward propagation of the MCC to the east of Mindanao Island. The magnitudes of ξ_{adv} and $\xi_{stretch}$ (Fig. 11c) are also comparable over the SCS and to the east of the Philippines. At Lag 0 (Fig. 11d to f), the magnitude of the $\xi_{stretch}$ (Fig. 11f) becomes

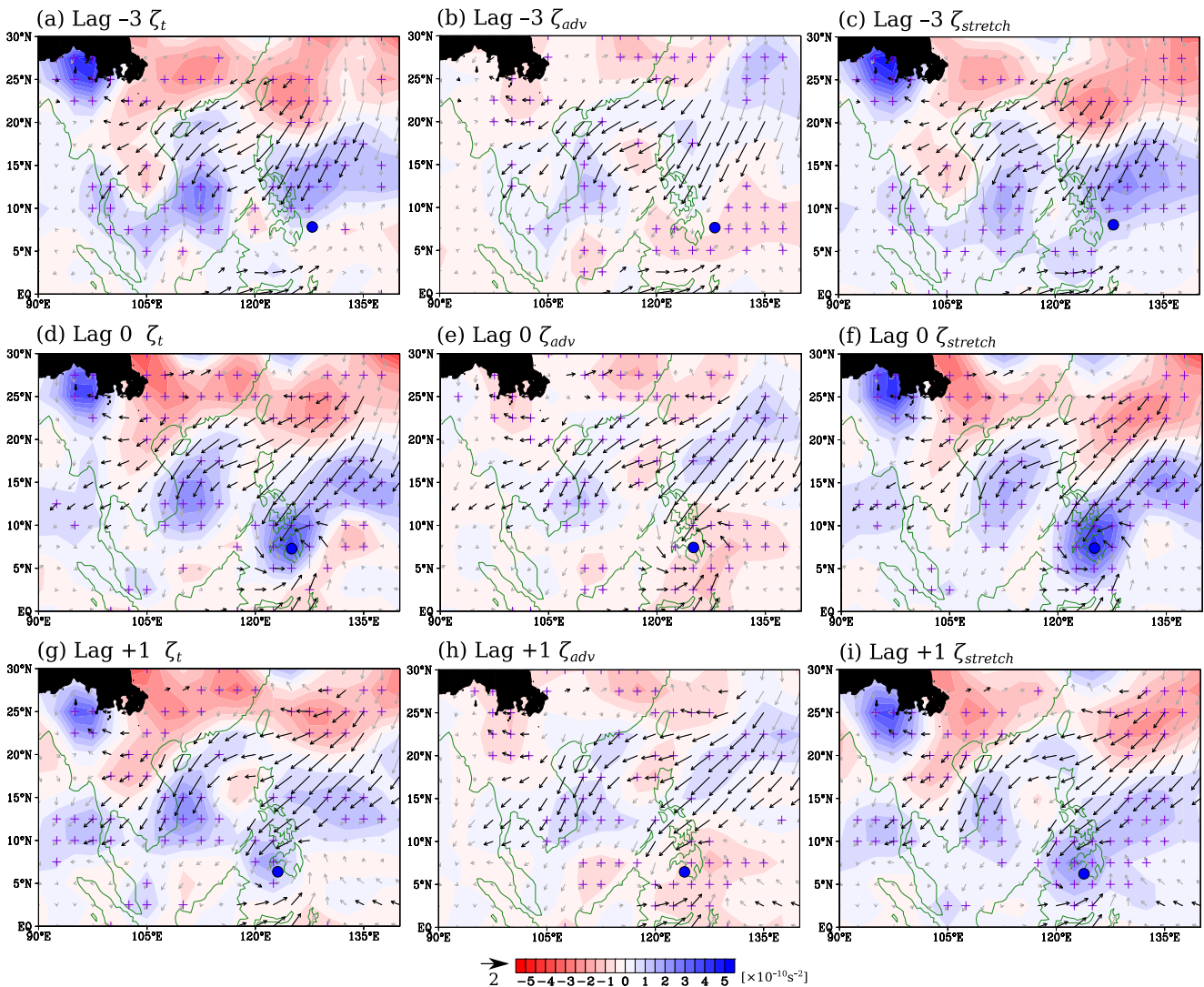


Fig. 11 Spatial distribution of composite anomalies of vorticity tendency (ζ_t ; $\times 10^{-10} \text{ s}^{-2}$), its advection term (ζ_{adv} ; $\times 10^{-10} \text{ s}^{-2}$), and stretching term ($\zeta_{stretch}$; $\times 10^{-10} \text{ s}^{-2}$) for Lag -3 (a, b, c); Lag 0 (d, e, f); and Lag +1 (g, h, i), respectively. The 925 hPa wind anomalies (m s^{-1}) are superimposed for discussion. The blue circle indicates the center of the anomalous

cyclonic circulation over Mindanao Island (MCC). Bold vectors and cross marking (+) indicate statistical significance at the 90 % confidence level using Student’s *t*-test. The scale of the wind vector is 2 m s^{-1}

larger than the ξ_{adv} (almost five times; Fig. 11e) and extends to the east of the Philippines. This inhibits the westward propagation of the cyclonic anomaly over Mindanao Island. This implies that the intensification of the MCC is mainly achieved by the vorticity stretching, which is facilitated by the enhanced low-level convergence over this area. The MCC starts its west/southwestward propagation when $\xi_{stretch}$ (Fig. 11i) weakens at Lag +1 together with the weakening of the southerly V_{925hPa} in Fig. 10a. On the other hand, the ξ_{adv} is positive to the west of the MCC, which favors the westward propagation. At Lag +3 (Fig. 12a to c), the MCC is located off the eastern coast of Borneo and centered around 120°E , 5°N . The ξ_{adv} (Fig. 12b) is positive to the west of the MCC while its magnitude is almost comparable to the $\xi_{stretch}$ (Fig. 12c). This still favors the westward propagation of the MCC. At Lag +5 (Fig. 12d to f), a

cyclonic circulation develops to the west of Borneo, while the center of the MCC weakens and becomes unclear. Positive $\xi_{stretch}$ can be depicted over the SCS. Another positive $\xi_{stretch}$ region can also be seen to the east of the Philippines around the confluence zone of the northeasterlies from the mid-latitudes and southerlies from the equatorial region. In the succeeding lag hours, the MCC dissipates and the magnitudes of both the $\xi_{stretch}$ and ξ_{adv} becomes comparable again (not shown).

5 Summary and Discussion

This study examined the climatology of the non-TC related winter heavy rainfall/flood events (HRF) from 1979 to 2017 over the Philippines through a case study and composite

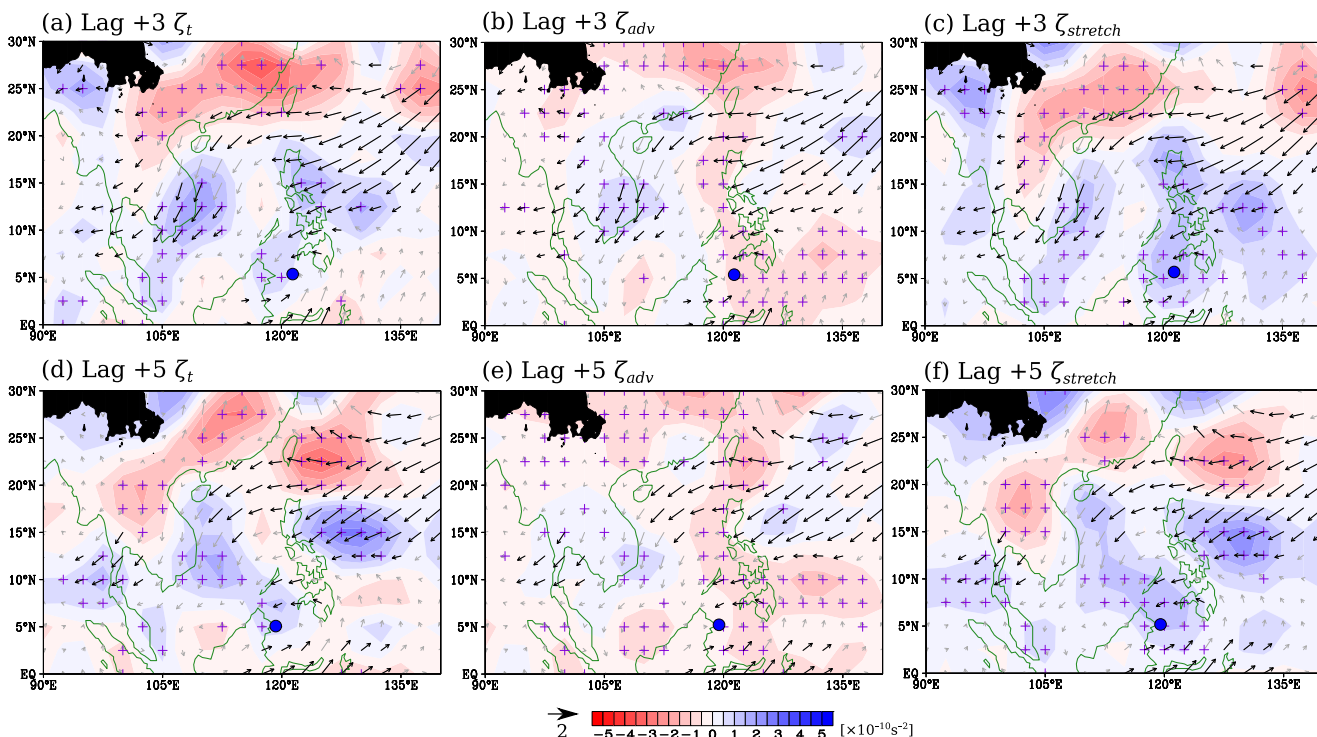


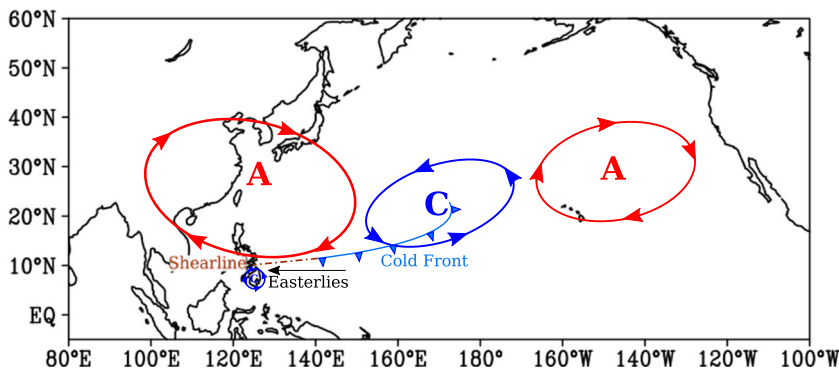
Fig. 12 As in Fig. 11 but for: Lag +3 (a, b, c); and Lag +5 (d, e, f)

analysis. The case study examined led to urban flooding (HRF) over Cagayan de Oro City (CDO) in Mindanao Island (122–127°E, 5–10°N), Philippines on January 16, 2017 (JAN2017 event). This HRF event is associated with the interaction of a westward propagating anomalous cyclonic circulation around Mindanao Island and a shearline that is associated with an anomalous eastward-propagating cyclonic circulation (i.e., cold front) along 20–40°N and its interaction with the tropical easterlies. The shearline can be identified as a region with enhanced moisture convergence and enhanced zonal wind gradient. The accumulated rainfall during this HRF event in one weather station by the Weather Philippines Foundation Incorporated over CDO from 00 UTC January 16 to 00 UTC January 17, 2017 is almost twice the climatological daily maximum rainfall for January over CDO. The maximum moisture convergence during this

event was found during 06 UTC January 16, 2017. Enhanced westerly U_{925hPa} and southerly V_{925hPa} during 06 UTC January 16, 2017 over Mindanao Island might have supplied more warm and humid tropical air that interacted with the cool and dry air from the enhanced northerly V_{925hPa} . This interaction resulted in enhanced moisture convergence and rainfall over Mindanao Island.

Using the flood reports archived by the Dartmouth Flood Observatory, we examined the climatology of non-TC related HRF events over the Philippines from 1979 to 2017. As previously noted, previous studies on non-TC related winter HRF events focused only on specific cases or carried out impact-based studies. Hence, this study is the first attempt to characterize these winter HRF events in a climatological mean sense. We identified 34 cases of such HRF events, 25 (74%) of which occurred over Mindanao Island; therefore, we only focused

Fig. 13 Schematic diagram of the possible mechanism leading to the winter HRF over Mindanao Island (southern Philippines). The cyclonic and anticyclonic circulations are denoted as “C” and “A”, respectively. The dot-dashed line indicates the location of the shearline



our analysis over Mindanao Island since most of the cases occurred over this region. Using the maximum area-averaged vertically integrated moisture flux convergence of the reported HRF event over Mindanao Island to represent the peak rainfall, we created composites to understand the mechanisms leading to these HRF events. A schematic diagram of the possible mechanism leading to the winter HRF over Mindanao Island is shown in Fig. 13.

The composites show that the winter HRF events over Mindanao Island is induced by the interaction of the eastward propagating cyclonic and anticyclonic circulation anomalies along 20–40°N and a westward propagating cyclonic anomaly along 5–10°N (i.e., the MCC), similar to the above mentioned January 2017 HRF event. A shearline is formed at the trailing end of the cold front associated with the eastward propagating anomalous cyclonic and anticyclonic circulations. The interaction of the shearline and the MCC induces HRF events over Mindanao Island. Composite analysis of the large-scale circulation features further revealed that the enhanced southerly V_{925hPa} in the south of Mindanao Island prevented the MCC from progressing southward despite the background northeasterlies. In addition, we also performed vorticity budget analysis to explain the westward propagation tendency of the MCC. We decomposed the vorticity tendency into its advection and stretching terms. It turns out that the MCC only propagated westward when both the advection and stretching terms were comparable to each other, together with the weakening of the southerly V_{925hPa} . The enhanced convergence over Mindanao Island favored the enhancement of the stretching term, which inhibited the westward propagation of the MCC.

Yokoi and Matsumoto (2008) found the importance of westward propagating TDDs associated with an MJO-like convective activity over the maritime continent to the HRF over central Vietnam. Pullen et al. (2015) also found the role of MJO on the February 2008 HRF event over the Philippines. Using the Wheeler and Hendon (2004) index (hereafter, WHI) for depicting the location and strength of the MJO, we checked the WHI of the 25 cases over Mindanao Island. The WHI defines the MJO component based on a multivariate empirical orthogonal function (EOF) analysis of daily 850 hPa zonal wind, 200 hPa zonal wind, and Outgoing Longwave Radiation (OLR) between 15°S–15°N. Two principal component time series from the EOF analysis are defined as Real-time Multivariate MJO series 1 and 2, RMM1 and RMM2, respectively. The RMM1 and RMM2 are drawn in a phase-space diagram to indicate the magnitude and location of the MJO. The equatorial region is divided into 8 regions: South America to Africa (Phases 1 and 8), Indian Ocean (Phases 2 and 3), Maritime Continent (Phases 4 and 5), and the Pacific Ocean (Phases 6 and 7). Since the MJO propagates eastward, its trajectory on the

phase-space diagram is drawn counter-clockwise. The MJO is weak (strong) when the WHI is less (greater) than 1.

There were 12 HRF cases that occurred when the MJO phase is weak, including the JAN2017 case, and only two cases occurred when the MJO is over the maritime continent (not shown). The rest occurred when the MJO is located over the Indian Ocean or the western Pacific. These results suggest that not all winter HRF cases can be associated with MJO and that other factors might be involved. On the other hand, aside from the MJO, Compo et al. (1999) found that cold surges south of 25°N also have significant periodicities at the submonthly (i.e., 6–30-days) time scale. Takahashi et al. (2011) examined the impact of long lasting northerly cold surges at the submonthly time scale on the TC formation over the tropical region. They found that the long-lasting northerly surges may facilitate the formation of TCs over the SCS during October and November. The role of these intraseasonal northerly surges on the formation and development of the MCC will be discussed further in our future study. In addition, this study was limited by the availability of a long-term high temporal rainfall (and other variables) data set. Therefore, it would be interesting to extend the analysis when such data sets are already available in future studies. This study only examined the dynamical aspects of the HRF event. The thermodynamical aspects including the changes in the instability leading to the HRF event will be explored in future studies. Simulating these HRF events using numerical models for improved forecasting is also of great interest.

Acknowledgements Lyndon Mark Olaguera and Jun Matsumoto were supported by the Tokyo Human Resources Fund at Tokyo Metropolitan University from the Tokyo Metropolitan Government. Jun Matsumoto is supported by the Grant-in-Aid for Scientific Research (KAKENHI) No. 26220202 and 19H00562. This research was also supported by the Science and Technology Research Partnership for Sustainable Development (SATREPS) No. JPMJSA1612 funded by the Japan Science and Technology (JST) and Japan International Cooperation Agency (JICA), and the e-ASIA Joint Research Program, funded by JST. The authors are also grateful for the constructive comments from the editor and anonymous reviewers in further improving this manuscript.

Compliance with Ethical Standards

Conflict of Interest The authors declare no conflict of interest.

Open Access This article is licensed under a Creative Commons Attribution 4.0 International License, which permits use, sharing, adaptation, distribution and reproduction in any medium or format, as long as you give appropriate credit to the original author(s) and the source, provide a link to the Creative Commons licence, and indicate if changes were made. The images or other third party material in this article are included in the article's Creative Commons licence, unless indicated otherwise in a credit line to the material. If material is not included in the article's Creative Commons licence and your intended use is not

permitted by statutory regulation or exceeds the permitted use, you will need to obtain permission directly from the copyright holder. To view a copy of this licence, visit <http://creativecommons.org/licenses/by/4.0/>.

References

- Banacos, P.C., Schultz, D.M.: The use of moisture flux convergence in forecasting convective initiation: historical and operational perspectives. *J. Clim.* **20**, 351–366 (2005)
- Cabanerit, J.: Interaction between a Shearline and the Inter-Tropical Convergence Zone in Northwestern Coast of Venezuela (25 November Heavy Rainfall Event), (2016). Available at: https://www.wpc.ncep.noaa.gov/international/internal/PRESENTATIONS/ID_201607_Julio_Cabanerit_Venezuela.pdf. Accessed 6 Dec 2019
- Cayan, E.O., Chen, T.C., Argete, J.C., Yen, M.C., Nilo, P.D.: The effect of tropical cyclones on southwest monsoon rainfall in the Philippines. *J. Meteorol. Soc. Jpn.* **89**, 123–139 (2011)
- Chen, T.C.: Global water vapor flux and maintenance during FGGE. *Mon. Weather Rev.* **113**, 1801–1819 (1985)
- Chen, T.C., Tsay, J.D., Yen, M.C., Matsumoto, J.: Interannual variation of the late fall rainfall in Central Vietnam. *J. Clim.* **25**, 392–413 (2012)
- Chen, T.C., Tsay, J.D., Yen, M.C., Matsumoto, J.: The winter rainfall of Malaysia. *J. Clim.* **26**, 936–958 (2013)
- Chen, T.C., Tsay, J.D., Matsumoto, J., Alpert, J.: Development and formation mechanism of the southeast Asian winter heavy rainfall events around the South China Sea. Part I: Formation and propagation of cold surge vortex. *J. Clim.* **28**, 1417–1443 (2015a)
- Chen, T.C., Tsay, J.D., Matsumoto, J., Alpert, J.: Development and formation mechanism of the southeast Asian winter heavy rainfall events around the South China Sea. Part II: Multiple interactions. *J. Clim.* **28**, 1444–1464 (2015b)
- Christidis, N., Betts, R.A., Stott, P.A.: The extremely wet March of 2017 in Peru. *Bull. Am. Meteorol. Soc.* **100**, S31–S35 (2019)
- Cinco, T.A., de Guzman, R.G., Hilario, F.D., Wilson, D.M.: Long-term trends and extremes in observed daily precipitation and near surface air temperature in the Philippines for the period 1951–2010. *Atmos. Res.* **145**, 12–26 (2014)
- Cinco, T.A., de Guzman, R.G., Ortiz, A.M.D., Delfino, R.J.P., Lasco, R.D., Hilario, F.D., Ares, E.D.: Observed trends and impacts of tropical cyclones in the Philippines. *Int. J. Climatol.* **36**, 4638–4650 (2016)
- Compo, G.P., Kiladis, G.N., Webster, P.J.: The horizontal and vertical structure of the east Asian winter monsoon pressure surges. *Q. J. R. Meteorol. Soc.* **125**, 29–54 (1999)
- Cruz, F.T., Narisma, G.T., Villafuerte II, M.Q., Chua, K.C., Olaguera, L.M.: A climatological analysis of the southwest monsoon rainfall in the Philippines. *Atmos. Res.* **122**, 4638–4650 (2013)
- Faustino-Eslava, D.V., Yumul Jr., G.P., Servando, N.T., Dimalanta, C.B.: The January 2009 anomalous precipitation associated with the “tail-end of the cold front” weather system in northern and eastern Mindanao (Philippines): natural hazards, impacts, and risk reduction. *Glob. Planet. Chang.* **76**, 85–94 (2011)
- Hoell, A., Perlwitz, J., Dewes, C., Wolter, K., Rangwala, I., Quan, X.W., Eischeid, J.: Anthropogenic contributions to the intensity of the 2017 United States northern Great Plains drought. *Bull. Am. Meteorol. Soc.* **100**, S19–S24 (2019)
- Huffman, G.J., Adler, R.F., Bolvin, D.T., Nelkin, E.J.: The TRMM multi-satellite precipitation analysis (TMPA). In satellite rainfall applications for surface hydrology pp. 3–22. Springer, Dordrecht. (2010)
- Japan International Cooperation Agency: Preparatory survey for the project for improvement of flood forecasting and warning system for Cagayan de Oro river basin in the Republic of the Philippines, Report, pp. 1 (2018)
- Kanamitsu, M., Ebisuzaki, W., Woollen, J., Yan, S.K., Hnilo, J.J., Fiorino, M., Potter, G.L.: NCEP-DOE AMIP-II reanalysis (R-2). *Bull. Am. Meteorol. Soc.* **83**, 1631–1643 (2002)
- Kubota, H., Shirooka, R., Matsumoto, J., Cayan, E.O., Hilario, F.D.: Tropical cyclone influence on the long-term variability of the Philippines summer monsoon onset. *Prog. Earth Planet. Sci.* **4**, 27 (2017)
- Olaguera, L.M., Matsumoto, J., Kubota, H., Inoue, T., Cayan, E.O., Hilario, F.D.: Abrupt climate shift in the mature rainy season of the Philippines in the mid-1990s. *Atmosphere*, **9**, 350 (2018)
- Pullen, J.A., Gordon, L., Flatau, M., Doyle, J.C., Villanoy, C., Cabrera, O.: Multiscale influences on extreme winter rainfall in the Philippines. *J. Geophys. Res. Atmos.* **120**, 3292–3309 (2015)
- Stocker, T.F., Qin, D., Plattner, G.K., Tignor, M., Allen, S.K., Boschung, J., Nauels, A., Xia, Y., Bex, B., Midgley, P.M.: The physical science basis: contribution of Working Group I to the Fifth Assessment Report of the Intergovernmental Panel on Climate Change. Cambridge University Press, Cambridge United Kingdom and New York, USA, 1535 pp (2013).
- Takahashi, H.G., Fukutomi, Y., Matsumoto, J.: The impact of long-lasting northerly surges of the east Asian winter monsoon on tropical cyclogenesis and its seasonal march. *J. Meteorol. Soc. Jpn.* **89**, 181–200 (2011)
- Utsumi, N., Kim, H., Seto, S., Kanae, S., Oki, T.: Climatological characteristics of fronts in the western North Pacific based on surface weather charts. *J. Geophys. Res. Atmos.* **119**, 9400–9418 (2014)
- Villafuerte II, M.Q., Matsumoto, J., Akasaka, I., Takahashi, H.G., Kubota, H., Cinco, T.A.: Long-term trends and variability of rainfall extremes in the Philippines. *Atmos. Res.* **137**, 1–13 (2014)
- Villafuerte II, M.Q., Matsumoto, J., Kubota, H.: Changes in extreme rainfall in the Philippines (1911–2010) linked to global mean temperature and ENSO. *Int. J. Climatol.* **35**, 2033–2044 (2015)
- Wheeler, M.C., Hendon, H.H.: An all-season real-time multivariate MJO index: development of an index for monitoring and prediction. *Mon. Weather Rev.* **132**, 1917–1932 (2004)
- Yokoi, S., Matsumoto, J.: Collaborative effects of cold surge and tropical depression-type disturbance on heavy rainfall in Central Vietnam. *Mon. Weather Rev.* **136**, 3275–3287 (2008)
- Yumul, G.P., Dimalanta, C.B., Servando, N.T., Cruz, N.A.: Abnormal weather events in 2009, increased precipitation and disastrous impacts in the Philippines. *Climate Change*, **118**, 715–727 (2013)

Publisher's Note Springer Nature remains neutral with regard to jurisdictional claims in published maps and institutional affiliations.

